



**HAL**  
open science

## Durability of mortars with leftover recycled sand

Manh Tan Le, Christelle Tribout, Gilles Escadeillas

► **To cite this version:**

Manh Tan Le, Christelle Tribout, Gilles Escadeillas. Durability of mortars with leftover recycled sand. Construction and Building Materials, 2019, 215, pp.391-400. 10.1016/j.conbuildmat.2019.04.179 . hal-02165366

**HAL Id: hal-02165366**

**<https://insa-toulouse.hal.science/hal-02165366v1>**

Submitted on 22 Oct 2021

**HAL** is a multi-disciplinary open access archive for the deposit and dissemination of scientific research documents, whether they are published or not. The documents may come from teaching and research institutions in France or abroad, or from public or private research centers.

L'archive ouverte pluridisciplinaire **HAL**, est destinée au dépôt et à la diffusion de documents scientifiques de niveau recherche, publiés ou non, émanant des établissements d'enseignement et de recherche français ou étrangers, des laboratoires publics ou privés.



Distributed under a Creative Commons Attribution - NonCommercial 4.0 International License

# 1 Durability of mortars with leftover 2 recycled sand

3 Manh Tan LE <sup>a\*</sup>, Christelle TRIBOUT <sup>a</sup>, Gilles ESCADEILLAS <sup>a</sup>

4 <sup>a</sup> Université de Toulouse, UPS, INSA; LMDC (Laboratoire Matériaux et Durabilité des  
5 Constructions), 135, Avenue de Rangueil; F-31 077 Toulouse Cedex 04, France

6 \* Corresponding author. Tel +33665087813; E-mail address: mtle@insa-toulouse.fr

7

## 8 1. Introduction

9 Concrete is the most widely used material in construction. However, it has a negative impact on  
10 the environment due to the consumption of non-renewable resources (rocks for cement and  
11 aggregates, oil to produce the energy needed to manufacture it), production of greenhouse gases  
12 during cement production (about 1 ton of CO<sub>2</sub> per ton of clinker) and waste during its  
13 manufacture. For environmental and also economic reasons, it is becoming urgent to reduce the  
14 environmental impacts of concretes by reducing or optimizing wastes at the manufacturing stage.  
15 Such is the aim of this research.

16 Most concretes used on construction sites are made with ready mixed concrete manufactured in a  
17 concrete batching plant. A manufacturer produces about 40,000 m<sup>3</sup> of fresh concrete annually [1].  
18 These concretes are transported from the plant to the construction site by mixer truck. If too  
19 much concrete is ordered, the leftover concrete is returned to the factory and goes to waste. The  
20 fresh concrete that becomes waste in Europe is estimated at 1-4% of the total amount of concrete  
21 processed, depending on the location or region [2]. Within the EU, 234 million m<sup>3</sup> of ready-mix  
22 concrete was produced in 2013. With a return rate of 3%, the amount of leftover ready-mix  
23 totaled 7 million m<sup>3</sup>/year, with a value of 466.2 million euros [3]. This means that the residual  
24 concrete of each ready-mix plant is 1,600 m<sup>3</sup> per year, or around 4,000 tons of concrete. The cost  
25 of storing and processing such amounts is also huge. Therefore, it is necessary to find sustainable  
26 recovery solutions for this concrete.

27 Currently, the profession uses two solutions for residual concrete. The first is to wash the concrete  
28 returns, to separate the aggregates and loaded water. Aggregates can be reused for road building

1

29 and the loaded water is used for the next production of concrete. The second solution is to dump  
30 the returns in skips, leave this residual concrete to cure for a few days and then crush it (Figure 1).  
31 In this study, the residual concrete is treated by the second solution.

32 Although large aggregates (gravel) can be reused without difficulty [4], the same cannot be said  
33 for fine aggregates (sand). Evangelista et al. [5] show that recycled sand (RS) has characteristics  
34 and behavior that are very different from those of natural sand. Because of the way it is produced,  
35 the shape of RS is irregular, apparently with high roughness and surface area. Moreover, its  
36 mineralogical composition is very rich in calcium or siliceous oxide and cement. Obviously, the  
37 layer of hydrate absorbs water. Zhao et al. [6, 7] show that the quantity of linked hydrate in the RS  
38 is different for each fraction and, consequently, the water absorption coefficient of the RS is also  
39 different. Some research has focused on modeling to find a method for determining the water  
40 absorption coefficient of each fraction [6, 8]. The newly developed and traditional methods (NF EN  
41 1097-6) give very similar results for the fraction larger than or equal to 0.8 mm. However, for the  
42 fraction smaller than 0.8 mm, the methods give very different values. The workability of mortar is  
43 also strongly influenced by the moisture condition of the RS. Remond et al. [9] show that the time  
44 necessary to obtain moisture equilibrium in the pre-saturation state is above 7 days.

45 When the RS is substituted in the mortar, the strength of the mortar can drop by as much as 60%  
46 of the initial value for mortar without RS [10]. Zhao et al. [6] show an important influence of the  
47 finest fraction (less than 0.63 mm) of the RS since it engenders the most penalizing effect on the  
48 mechanical properties of mortars.

49 Although there are still problems, the performance of the concrete may be acceptable for some  
50 ways of valorization. The mechanical performance is low and presents uncertainty but use is  
51 possible in some cases. For sustainable use, it is also necessary to study the durability of mortars in  
52 which RS is incorporated.

53 The work presented here mainly studied RS durability. Many indicators of durability were  
54 considered (air permeability, chloride ion migration, capillarity, carbonation and porosity  
55 accessible to water) according to the mortar composition. The results were compared with those  
56 for reference mortars made with natural sand. In order to take account of the fact that outside  
57 storage of this young concrete leads to its carbonation, two series of mortars were formulated by  
58 replacing natural sand (NS) with either non-carbonated recycled sand (RS) or carbonated recycled

59 sand (CRS). We know that natural carbonation is a very slow process. Recycled aggregates,  
60 especially fine parts, incorporate portlandite and hydrated silicates that can be carbonated faster  
61 than concrete in structures. A French national project named FastCarb [11] is dealing with the  
62 study of the accelerated carbonation. Started in 2018, its aim is to store CO<sub>2</sub> in “recycled concrete  
63 aggregates” in an accelerated manner, to improve the quality of these aggregates by blocking the  
64 porosity and, ultimately, to reduce the CO<sub>2</sub> impact of concrete in structures.

## 65 **2. Materials and methods**

### 66 **2.1 Materials**

#### 67 **2.1.1 Sands**

68 The leftover concrete was formulated with siliceous aggregates and CEM I or II as is usually done in  
69 the region of Toulouse, France. This remaining concrete had been dumped and left to harden.

70 After crushing in industrial conditions, the recycled aggregates were stored in closed bags to  
71 prevent supplementary carbonation. These aggregates were sieved with a 4 mm mesh in order to  
72 keep only the sand fraction, which was dried at 80°C to constant mass.

73 Three sands were used:

- 74 - a non-carbonated **Recycled Sand (RS)**. For some parts of this study, the RS was divided into  
75 3 fractions: Fine (f) - 0/0.25 mm, Medium (m) - 0.25/1 mm and Coarse (c) - 1/4 mm;
- 76 - a **Carbonated Recycled Sand (CRS)** obtained by placing the RS in an accelerated  
77 carbonation chamber with 50% CO<sub>2</sub> and 60% RH for 1 week. CRS was studied only on the  
78 total range of 0/4 mm;
- 79 - a **Natural Sand (NS)**, rounded, with the petrographic nature of silica sand, grading 0/4 mm.  
80 As for RS in some parts of this study, the NS was also divided into 3 fractions Fine (f),  
81 Medium (m) and Coarse (c).

82 The particle size distributions of NS and RS are shown in Fig 2. The NS curve is typical of the natural  
83 river sands of the Toulouse region of France. The RS and CRS curves are typical of crushed sands  
84 and particularly of sand from crushed mortar [9]. CRS is simple RS that has been carbonated,  
85 which changes its chemical composition but not its shape. Thus, particle size distributions of RS  
86 and CRS were similar and only the RS curve is presented.

87 Fig 3 gives the water absorption coefficient (WA) of the studied sands, determined with the  
88 standard method 1097-6 [12]. RS has the largest value with 12.5% WA, followed by CRS with 8.1%,  
89 and NS with 1.2%. The presence of old cement paste in RS induces an increase of about 10% of  
90 WA, compared to NS. The WA of CRS decreases with respect to RS due to calcium carbonate  
91 precipitation, which appears during the carbonation of portlandite and C-S-H. This new  
92 component increases the volume of the solid and reduces porosity and WA [13].

93 Fig 3 also shows the WA results for different grades. WA is higher when the grain size is small, for  
94 both NS and RS. The WA in fine fraction  $RS_f$  is about 9 times higher than that of  $NS_f$  and the same  
95 proportions are found for the medium fractions,  $RS_m$  and  $NS_m$ . For the two coarsest fractions,  $RS_c$   
96 and  $NS_c$ , WA is about 12 times higher in  $RS_c$ . This high value of WA is in accordance with the results  
97 obtained by Zhao et al. [6, 7, 10]. Pore structure and the amount of bound cement paste can  
98 explain this high value of WA in RS in comparison with NS. In the RS, the bound cement paste  
99 leads to increased porosity and induces water absorption. It can also be noted that there are some  
100 difficulties in determining the WA value of fine fraction [6]. This fraction contains smaller grains or  
101 cement with a large water absorption capacity, so there is a greater risk of some interstitial water  
102 being present between the grains. That could explain the higher uncertainty associated with  $RS_f$ .

103 Fig 4 shows the real density and the absolute density of the three sands: NS, RS and CRS. The real  
104 density test was also performed with the 1097-6 standard method [12]. The absolute density  
105 results were compiled by hydrostatic weighing, according to standard NF EN 1097-7 [14], of a  
106 sample crushed above 80  $\mu\text{m}$  and placed in a vacuum. The absolute density is maximal with the NS  
107 ( $2.70 \text{ g/cm}^3$ ) and lower in RS or CRS. The real density was lower ( $2.62$ ,  $2.01$  and  $2.20 \text{ g/cm}^3$  for NS,  
108 RS and CRS respectively), particularly for RS and CRS. The difference between real density and  
109 absolute density for RS and CRS comes from the porosity of the old cement paste present in RS  
110 and CRS sands. The more the older cement paste is present, the greater the volume of porosity is.  
111 This increase of porosity induces a decrease of the real density. The RS has more old cement  
112 paste, more pores and lower real density. In the case of CRS, the carbonation induces a filling of  
113 the pores and consequently the real density of CRS is higher than that of the corresponding RS.

114 Fig 4 also gives the density of each fraction of the NS and RS. When the standard deviation is taken  
115 into account, densities of the NS are the same for all fractions because of its homogeneous  
116 composition, whereas there are large variations between the fractions of the RS, which become  
117 even greater as the fractions become finer. A large standard deviation is observed in the  $RS_f$

118 fraction in comparison with other fractions. All differences can only come from the cementitious  
119 matrix present in the RS, which constitutes a large proportion of the fine fraction, as has already  
120 been shown with the SEM images.

121 Both WA and density can be used to classify the aggregates according to Silva et al. [15] which  
122 propose a generic prediction model with these parameters, regardless of their size, type and  
123 origin: CII for RS and BIII for CRS (Fig 5).

## 124 **2.1.2 Cement**

125 The cement used was ordinary Portland cement CEM I 52.5 R as specified in European Standard EN  
126 197-1 [16]. This cement, produced by Lafarge, La Malle (France), has a density of  $3.15 \text{ g/cm}^3$  and  
127 Blaine fineness of  $4300 \text{ cm}^2/\text{g}$ . Its chemical and mineralogical composition is given in Table 1.

## 128 **2.1.3 Mortars**

### 129 **2.1.3.1 Formulation**

130 Two series of mortars were studied: the RS and CRS series. RS and CRS were made by replacing NS  
131 by RS at 4 rates (0, 33, 66 and 100%).

132 The formulations of the three series of mortars were based on four principles:

- 133 - NS was replaced by the same volume of RS or CRS ( $650 \text{ l/m}^3$ );
- 134 - The same amount of effective water was used (222 l);
- 135 - The quantity of cement (CEM I 52.5 R) used throughout was fixed at  $333 \text{ kg/m}^3$ ;
- 136 - An air volume of  $22 \text{ l/m}^3$  was taken into account for all formulations.

137 The formulations are presented in Table 2.

138 The mortars were cast according to standard EN 196-1 [17]. The dry sands were pre-saturated 24  
139 hours before casting with a quantity of water corresponding to their WA, placed in sealed bags  
140 and then stored in an air-conditioned room at  $20 \pm 2 \text{ }^\circ\text{C}$ . As the sand had been pre-saturated, the  
141 amount of water added in the mixer corresponded to the effective water.

142 Two kinds of geometric shapes were used according to the test standards: cylinders (diameter ( $\phi$ )  
143 11 cm, height (H) 22 cm) for durability tests, and prisms (4x4x16 cm), for strength and carbonation  
144 tests. After casting, the samples were covered and placed in the humidity chamber at  $20 \text{ }^\circ\text{C}$  and  
145 more than 90% RH, demolded one day after pouring and then stored in water at  $20 \text{ }^\circ\text{C}$  until the  
146 date of the test.

147 **2.2 Methods**

148 **2.2.1 Workability**

149 To measure the consistency of mortars, a workability test was performed according to standard NF  
150 P 18-452 [18]. The test was performed immediately after mixing (between 1 and 3 minutes after).

151 **2.2.2 Apparent specific mass**

152 The density of the fresh mortar was measured according to standard NF EN 12350-6 [19].

153 **2.2.3 Strength**

154 Compressive strength testing [17] was performed on all specimens with a constant stress rate (2.4  
155 kN/s) controlled by the mortar press in the laboratory. The compressive strength test was  
156 conducted at 2, 7 and 28 days. At each date, 2 specimens were tested in flexion and 4 half  
157 specimens in compression.

158 **2.2.4 Durability tests**

159 At 21 days, two cylindrical samples of each composition were sawn into five parts: three with a  
160 thickness of  $50 \pm 1$  mm and two of  $20 \pm 1$  mm. A 10 mm section was excluded at each end.  
161 Samples were then put back into humid conditions [NF EN 12390-2 [20]] until the test, which took  
162 place at 28 days.

163 **2.2.4.1 Porosity accessible to water and Density**

164 For each composition, four  $\phi 110 \times H 20$  mm specimens were saturated under vacuum for 24 hours  
165 and dried at  $105^\circ\text{C}$  to constant mass. This test is defined in standard NF EN 18-459 [21].

166 **2.2.4.2 Chloride ion migration**

167 The test was performed according to the NT BUILD 492 method [22]. The catholyte solution was  
168 10% NaCl by mass in tap water and the anolyte solution was 0.3 mol/l NaOH in distilled water. The  
169 temperature of the sample and solutions was maintained at  $20^\circ\text{C}$  during the test. Three  
170  $\phi 110 \times H 50$  mm specimens were tested, under a voltage of 10 V for 24 hours.

171 **2.2.4.3 Air permeability**

172 After 28 days in humid conditions, three  $\phi 110 \times H 50$  mm specimens were placed at  $105^\circ\text{C}$  until the  
173 date of the air permeability test. The test was performed according to XP P18-463 [23] with a  
174 CEMBUREAU apparatus. The specimens were placed in a constant gas pressure gradient after 28

175 days at 80°C and in the dry state. The permeability was determined by measuring the gas flow  
176 through them.

#### 177 *2.2.4.4 Capillarity*

178 This test was performed on the samples that had been used for the air permeability test. In  
179 accordance with standard EN 772-11 [24], samples were immersed in water to a maximum height  
180 of 3 mm, which was obtained by using shims. At each time, the specimens were removed from the  
181 container, wiped with a paper towel, weighed, and then replaced in the container. The capillarity  
182 was measured at 0.25, 0.5, 1 and 2 hours.

#### 183 *2.2.4.5 Carbonation*

184 The carbonation test was performed according to standard NF XP P18-458 [25]. After 28 days in  
185 water, two 4x4x16 cm specimens were placed at 40 °C for a week and put into a chamber with 4%  
186 CO<sub>2</sub> and 65% HR. A 2 cm sample was sawn at each date: 3, 7, 14 and 28 days. The carbonated  
187 concrete thickness was measured after wetting the samples and spraying phenolphthalein  
188 solution on the fracture surfaces of the samples considered. Phenolphthalein solution reveals the  
189 interface between the safe (pH > 9) and the carbonated zone (pH < 9) by color difference.

### 190 **3. Results and discussion**

#### 191 *3.1 Characterization of the sands*

192 The amount of cement paste in the different fractions was observed by SEM. Figure 6 presents  
193 SEM images with EDS analyses for fractions RS<sub>f</sub> and RS<sub>c</sub>, which were respectively the finest and the  
194 coarsest. The siliceous mapping shows the place of siliceous aggregates. The calcium mapping,  
195 linked to the paste content, shows that more cement paste is present in RS<sub>f</sub>. This observation is in  
196 accordance with the findings of Evangelista et al. [5]. For the RS<sub>c</sub> fraction, the coarse aggregates  
197 are surrounded by only a thin layer of calcium. So, when the grain size is smaller, the amount of  
198 paste linked is greater, which also explains the tendency of the water absorption coefficient  
199 presented before.

200 Cement content was determined by soluble and insoluble methods [26]. Both methods led to  
201 similar results: 29-30% for RS<sub>f</sub>; 21-22% for RS<sub>m</sub> and 16-17% for RS<sub>c</sub>, the highest content being  
202 found for the RS<sub>f</sub> fraction, as expected.



203 These results were also confirmed by thermogravimetric results (Table 3). The sample was put in  
204 an argon atmosphere and subjected to a rise of temperature 10°C/min. The C-S-H mass loss was  
205 6.2 %; 4.4% and 3.3 % for RS<sub>f</sub>, RS<sub>m</sub> and RS<sub>c</sub> fractions, respectively. Portlandite was less present in  
206 the RS fraction, in a range of 0.6-1% of the total. The calcium carbonate rate was high, with 8.6%;  
207 4.9% and 4.3% for RS<sub>f</sub>, RS<sub>m</sub> and RS<sub>c</sub> fractions, respectively.

208 Thus, the main differences in chemical and physical properties between RS and NS were  
209 determined. The RS is surrounded by a layer of hydrates, mainly compounds with C-S-H, calcium  
210 carbonate and portlandite. This layer increases the porosity of the RS, thus increasing its water  
211 absorption coefficient. The distribution of the old cement paste in the RS is non-homogeneous  
212 since it depends on the grain size. Fine parts like RS<sub>f</sub> contain more cement paste.

213 The RS and CRS can strongly influence the mortar properties because of their structural and  
214 chemical differences compared to NS. The next part of the study explains how these modifications  
215 can influence the mortar properties and durability.

## 216 3.2 Characterization of the mortars

### 217 3.2.1 Workability

218 The workability of RS and CRS series is shown in Fig 7. Workability increases with the percentage  
219 of RS whatever the kind of mixture, a fact that could be explained by the presence of an excess of  
220 effective water due to the difficulty of determining the true amount of absorbed water [6]. The  
221 reduction of the time could also be explained by the fact that RS is lighter than NS (see Fig 4) and  
222 leads to an easier mortar flow. In addition, the old cement paste layer bound to the aggregates in  
223 RS makes this sand smoother than NS. Some of the absorbed water was able to migrate into the  
224 mortar during the vibration period [27].

### 225 3.2.2 Apparent specific mass

226 Figure 8 shows the fresh density of the RS and CRS mortars with all substitution rates. It can be  
227 seen that the density of mortars decreases with the rate of replacement by RS or CRS.

228 If these experimental densities are compared with the theoretical densities calculated from the  
229 formulations (Table 2), the experimental values are the same for RS replacement if we take the  
230 dispersion into account. A difference for CRS mixtures (+25 l) can be observed, which could be  
231 explained by more air content.

### 232 **3.2.3 Compressive strength**

233 Figure 9 presents the results of the compressive strength test at 2, 7 and 28 days for the RS and  
234 CRS series.

235 In all cases, the mortar RS0 shows the best performance and strength decrease with the rate of  
236 replacement of sand. The more NS is replaced, the greater the resistance drop since the resistance  
237 of the old cement paste layer around the aggregates of RS is weaker than that of NS aggregates  
238 alone.

239 For the RS series, the maximal decrease for a total replacement is 28%, 22% and 26% respectively  
240 at 2, 7 and 28 days. These results were also found by Zhao et al. [6], who reported that mortar  
241 made with 100% replacement with RS showed a similar reduction rate to that of the reference  
242 mortar RS0. At 2 and 28 days, the performance of RS33 showed results very close to the reference  
243 (decrease of 8% and 3% respectively).

244 For the CRS series, the performance was higher than for the RS series. At 28 days, replacing 100%  
245 of NS by CRS induced a decrease of only 10%.

## 246 **3.3 Durability**

247 All durability results in the hardened state of RS and CRS mortars with different substitution rates  
248 are presented in Table 4.

### 249 **3.3.1 Density and Porosity**

250 The apparent density decreases with the replacement of NS by RS or CRS. Considering the  
251 dispersions, this could be explained by the fact that RS or CRS are lighter than NS.

252 For the RS and CRS series, the porosity accessible to water increases with the replacement rate.  
253 The presence of old paste around RS and CRS explains this tendency.

### 254 **3.3.2 Chloride ion diffusion**

255 The chloride ion migration coefficient for RS and CRS series is about  $10^{-11}$  m<sup>2</sup>/s, with good  
256 repeatability for all mixtures.

257 Two phenomena can lead to an increase in the diffusion coefficient: an increase of porosity or a  
258 drop in the chloride fixation capacity. For these mixtures, the two events are in competition. On  
259 the one hand, the more NS is replaced, the more the porosity increases, due to the presence of a

260 greater old paste content. On the other hand, when NS is replaced by RS or CRS, the quantity of  
261 old paste is increased to fix chloride (with formation of chloroaluminates). In the case of this  
262 study, the two effects cancel each other out.

### 263 **3.3.3 Air permeability**

264 The values of air permeability at 28 days and at the dried state for RS and CRS series increase in  
265 the same manner from 50 to 350.  $10^{-18} \text{ m}^2$  (repeatability is good for all mixtures). These results  
266 agree with porosity results (see 3.3.1) and the literature [25, 26].

### 267 **3.3.4 Capillarity**

268 The capillarity results show a classical square root progression versus time. The values of the  
269 slopes, representing the speed of capillarity, are only presented at 7 days in the table for the RS  
270 and CRS series (the 28 days results were similar).

271 The capillarity coefficient increases with the rate of RS or CRS substitution. The capillarity of the RS  
272 series is about twice that of the CRS series.

### 273 **3.3.5 Accelerated Carbonation**

274 As for the capillarity results, a near-linear evolution with the square root of time is observed. For  
275 the same reason as for capillarity, the results are presented as a speed of carbonation in Table 4.  
276 The results for RS and CRS mixtures are lower than the reference one. In this case also, two  
277 phenomena are in competition. On the one hand, the carbonation speed increases with the  
278 porosity. On the other hand, the carbonation speed decreases with the quantity of available  
279 carbonable products. This is the case when we replace NS by RS or CRS, due to the presence of old  
280 paste. In this study, the influence of carbonable products is greater than the influence of porosity.  
281 Also, this explanation can be valid to explain the slight difference between RS and CRS: the lower  
282 porosity of CRS compensates for the initial carbonation of the portlandite of these aggregates.

### 283 **3.3.6 Performance approach**

284 In order to highlight the effect of recycled sand in substitution of natural sand, durability indicators  
285 (I) were calculated as the ratios between the mortars under study (RS, CRS) and the reference  
286 mortar RS0. All the indexes were chosen to express the durability of the mixtures: an index higher  
287 than 1 [30] indicated that the studied performance was better than the reference one and  
288 consequently the durability was improved thanks to the presence of recycled sand.

289 These indicators were calculated using the following equations:

$$I_s = \text{Strength index} = \frac{\text{Strength with RS/CRS/FRS}}{\text{Strength of RS0}}$$

$$I_{Cl} = \text{Chloride ion migration index} = \frac{\text{Log(Chloride migration coeff of RS0)}}{\text{Log(Chloride migration coeff with RS/CRS/FRS)}}$$

$$I_{Poroso} = \text{Water porosity index} = \frac{\text{Porosity of RS0}}{\text{Porosity with RS/CRS/FRS}}$$

$$I_{Cap} = \text{Capillarity index} = \frac{\text{Capillarity coefficient of RS0}}{\text{Capillarity coeff with RS/CRS/FRS}}$$

$$I_{Perm} = \text{gas permeability index} \\ = \frac{\text{Log(Gas permeability at dried state of RS0)}}{\text{Log(Gas permeability at dried state with RS/CRS/FRS)}}$$

$$I_{Carbo} = \text{Carbonation index at 28 days} \\ = \frac{\text{Carbonation depth at 28 days of RS0}}{\text{Carbonation depth at 28 days with RS/CRS/FRS}}$$

290 Figs. 10 and 11 present the results of durability indices for the RS and CRS series, respectively.  
291 Each axis represents an indicator, as shown above. A bold black line represents the index equal to  
292 1, meaning that the performance of the mixture with recycled sands is equivalent to that of the  
293 reference with natural sand (RS0).

294 Generally, for both kinds of mixtures, the durability range is very close to that of the RS0 mixture.  
295 However, a marked increase in durability can be noted for the chloride ion migration index,  $I_{Cl}$ , of  
296 the CRS series.

297 The substitution of 66% or 100% of RS of CRS impacts the index values slowly.

298 It can also be underlined that CRS mixtures show performances equal to or even better than those  
299 of RS mixtures (better compressive strength indices, migration indices and carbonation indices).

### 300 3.4 Discussion

301 RS differ from NS mainly in that they are composed of two fractions of different natures: natural  
302 aggregates and the old cement paste attached to them. The physical properties of recycled  
303 aggregates are different from those of natural aggregates. In SEM images, the RS often appears  
304 angular and rough, which, according to Evangelista and Brito [31], leads to greater internal friction.

305 The link between decrease of density and strength can help to predict results for other  
306 formulations. Fig. 12 presents the relation between the strength of hardened mortar and the  
307 decrease of density when NS is replaced by RS and CRS. The linear relationship between decrease  
308 of density and compressive strength is observed for both series, with good correlations in the case  
309 of CRS and acceptable ones for RS. This linear relation between density and strength in the case of  
310 recycled sand can also be found in the work of Tahar et al. [32].

311 The more NS is replaced by RS, the lower is the density and also the compressive strength. The  
312 CRS series has the lowest slope, about 4 or 5 times lower than the RS series. This series loses less  
313 strength than the others when NS is replaced. These results agree with the aggregate ranking  
314 proposed by Silva et al. [15] since RS (CII) ranks lower than CRS (BIII). This could be explained by  
315 the improvement of the quality of CRS aggregates with carbonation. The role of interfacial  
316 transition zone (ITZ) can be used to explain the compressive strength. In fact, by reducing the  
317 water absorption and the porosity, especially by the formation of carbo-aluminates, we provide a  
318 stronger ITZ so the compressive strengths are improved [36-38].

319 Figure 13 presents different models of the three sands, NS, RS and CRS. The NS is presented as  
320 rounded particles, the RS is rough and is presented as one or more NS particles within a layer of  
321 old cement paste, and the CRS is the same as RS but the old cement paste is carbonated and is  
322 shown in darker gray.

323 The angular shape and the bound old cement paste layer are the main causes of the variation in  
324 the characteristics of the recycled aggregates: decrease in density and increase in water  
325 absorption. Numerous studies have confirmed the results for these characteristic [36]–[40].  
326 Carbonation does not modify the granulometry of the sand but, by absorbing  $\text{CO}_2$ , the CRS  
327 becomes about 10% denser than RS (Fig 8) and its water absorption coefficient decreases from  
328 12.5% to 8.1%.

329 Thus, the presence of old cement paste in the recycled aggregates modifies their chemical  
330 characteristics relative to those of the natural aggregates. The cement content of the sand  
331 depends on the crushing cycle of the concrete and is directly related to the size of the aggregate  
332 [38]. Using two different methods, we observed the highest cement content for fraction  $\text{RS}_f$  and  
333 the lowest for fraction  $\text{RS}_c$ . Moreover, the characteristic of this layer depends directly on the origin  
334 of the recycled concrete [41].

335 Table 5 presents the variation of characteristics and durability for different sands (with total  
336 replacement of NS by RS or CRS). They are organized in three groups: group (1) shows the  
337 variation of characteristics between the fresh and hardened states (except for water absorption,  
338 which is the only criterion measured on the sands), and groups (2) and (3) show the variation of  
339 the mortar durability in the hard state. Group 2, with the porosity test, air permeability test and  
340 capillarity test, shows that durability is lowered, while group 3, with the carbonation test and  
341 chloride ion migration test, shows that durability is improved.

342 In group 1, although the water absorption is strong and reminds us that the sands were pre-  
343 saturated, the workability characteristic is good.

344 The results of group 2 are strongly influenced by the porosity of the sand. That is why the  
345 differences between results with RS and CRS are small. The high porosity creates more space in  
346 the structure of the mortar and less connection, thus decreasing the strength. However, Zhao et  
347 al. demonstrate that porosity is not the only factor influencing the compressive strength of mortar  
348 [42]. Capillary absorptions are significantly increased in the case of recycled aggregate mortars,  
349 due to a greater quantity of connected capillary pores [31], [43]. This high porosity is also a  
350 disadvantage for the air permeability. The more pores there are, the more easily the air can  
351 penetrate into the mortar.

352 In the mortar, 2/3 of the total volume is occupied by sand and 1/3 by cement paste. When 100%  
353 of natural sand is replaced by recycled sand, we can see an increase of mortar porosity (+14.9%)  
354 equivalent to the increase of granular porosity (+ 14.3%). For replacement of carbonated recycled  
355 sand, the difference between the increase of mortar porosity (+ 13.5%) and that of granular  
356 porosity (+9.6%) is more visible. A difference in air content, not measured in this study, could  
357 explain this result.

358 The results of group 3 are influenced not only by the porosity but also by the chemical  
359 composition of the sand. In this case, the important factor is the carbonation of old cement  
360 pastes. The carbonation of the recycled sand creates a volume of by-products that can block pores  
361 and decrease the penetration of CO<sub>2</sub>. With the chloride ion migration test, the aluminates and  
362 portlandite in the mortar capture the Cl<sup>-</sup> ions in solution to form chloroaluminates and calcium  
363 chloride, reducing the penetration of Cl<sup>-</sup>. Although improved resistance to chloride migration is  
364 observed with CRS, the use of RS does not have the same effect. The replacement of NS by RS

365 favors the propagation of chlorides. These phenomena are also found in the studies by Kou and  
366 Poon [31], and De Brito and Alves [34]. Abbas et al. [44] find diffusion coefficients of the same  
367 order of magnitude as those of traditional concretes.

## 368 **4. Conclusions**

369 In this paper, we looked for a way to add value to recycled sand from leftover concrete. We  
370 studied the influence of the partial or total substitution of natural sand (NS) by non-carbonated  
371 (RS) or carbonated recycled sand (CRS) in mortars following a performance approach. In the light  
372 of the tests results, the following conclusions can be drawn:

- 373 1. RS contain many hydrates and calcium carbonate in their structure. These hydrates lead to  
374 an increase in pore ratio and a decrease in density. They also lead to weaker material.
- 375 2. The cement content of this RS varied from 17 to 30% by mass according to the granular  
376 fractions, the highest value being observed in the fine fraction.
- 377 3. The characterization of recycled carbonated sand CRS showed that its porosity was lower  
378 than that of RS (32.9% instead of 34.3%).
- 379 4. The strength results were only slightly affected by substitution of NS by CRS (-5% for total  
380 replacement) whereas substitution of NS by RS was more unfavorable (-26% for total  
381 replacement).
- 382 5. The substitution of RS or CRS increases the porosity of mortar.
- 383 6. In dry conditions, the permeability of both RS100 and CRS100 tripled compared with that  
384 of RS0. Carbonation of RS had no great influence on the transport of air and there was no  
385 change between the RS and CRS series.
- 386 7. CRS presented favorable resistance to the migration of chloride, with a reduction of 66%  
387 for total replacement, whereas total substitution of NS by RS was unfavorable, with an  
388 increase of 36%.
- 389 8. A better tendency was observed for the carbonation result. The carbonation speed was  
390 reduced by about 25% when NS was replaced by RS or CRS.
- 391 9. The use of CRS could be very interesting. In order to generalize the conclusions, it would be  
392 necessary to study other recycled sands.

393

## 5. Acknowledgements

394 The authors wish to express their gratitude to the Granulab Company for providing the recycled  
395 sand used and for their financial support of this research.

396

## 6. References

- 397 [1] "Recyclage," *Solutions de traitement des rebuts de béton frais*. [Online]. Available:  
398 <http://bennerecyclagebeton.unblog.fr/environnement/>.
- 399 [2] L. de B. P. Vieira and A. D. de Figueiredo, "Evaluation of concrete recycling system efficiency  
400 for ready-mix concrete plants", *Waste Manag.*, vol. 56, pp. 337–351, Oct. 2016.
- 401 [3] "Ready mix concrete reclaimer and recycler, restbeton auswaschanlagen - Bibko GmbH."  
402 [Online]. Available: <http://www.bibko.com/en/>.
- 403 [4] M. Etxeberria, E. Vázquez, A. Marí, and M. Barra, "Influence of amount of recycled coarse  
404 aggregates and production process on properties of recycled aggregate concrete", *Cem. Concr.*  
405 *Res.*, vol. 37, no. 5, pp. 735–742, May 2007.
- 406 [5] L. Evangelista, M. Guedes, J. de Brito, A. C. Ferro, and M. F. Pereira, "Physical, chemical and  
407 mineralogical properties of fine recycled aggregates made from concrete waste", *Constr. Build.*  
408 *Mater.*, vol. 86, pp. 178–188, Jul. 2015.
- 409 [6] Z. Zhao, S. Rémond, D. Damidot, and L. Courard, "Une nouvelle méthode de caractérisation  
410 des granulats recyclés industriels: application aux mortiers", *2e édition de la Conférence*  
411 *Internationale Francophone: Nouveaux Matériaux et Durabilité*, Douai, France, Nov. 2015  
412 (Academic paper (PDF) accessible by ResearchGate).
- 413 [7] Z. Zhao, S. Rémond, D. Damidot, and W. Xu, "Teneur en pâte de ciment et coefficient  
414 d'absorption d'eau des sables recyclés", *15e édition des Journées Scientifiques du*  
415 *Regroupement Francophone pour la Recherche et la Formation sur le Béton*, Douai, France, July  
416 2014 (Academic paper (PDF) accessible by ResearchGate).
- 417 [8] V. W. Y. Tam, X. F. Gao, C. M. Tam, and C. H. Chan, "New approach in measuring water  
418 absorption of recycled aggregates", *Constr. Build. Mater.*, vol. 22, no. 3, pp. 364–369, Mar.  
419 2008.
- 420 [9] T. Le, S. Rémond, G. Le Saout, and E. Garcia-Diaz, "Fresh behavior of mortar based on recycled  
421 sand – Influence of moisture condition", *Constr. Build. Mater.*, vol. 106, pp. 35–42, Mar. 2016.
- 422 [10] Z. Zhao, S. Remond, D. Damidot, and W. Xu, "Influence of fine recycled concrete aggregates  
423 on the properties of mortars", *Constr. Build. Mater.*, vol. 81, pp. 179–186, April 2015.
- 424 [11] *FastCarb*, "Accueil", [Online]. Available: <https://fastcarb.fr/>.
- 425 [12] NF EN 1097-6, "Tests for mechanical and physical properties of aggregates — Part 6:  
426 Determination of particle density and water absorption", Jan. 2014.
- 427 [13] J. Zhang, C. Shi, Y. Li, X. Pan, C.-S. Poon, and Z. Xie, "Influence of carbonated recycled  
428 concrete aggregate on properties of cement mortar", *Constr. Build. Mater.*, vol. 98, pp. 1–7,  
429 Nov. 2015.



- 430 [14] NF EN 1097-7, "Tests for mechanical and physical properties of aggregates — Part 7:  
431 Determination of the particle density of filler — Pycnometer method", Jun. 2008.
- 432 [15] R. V. Silva, J. de Brito, and R. K. Dhir, "Properties and composition of recycled aggregates  
433 from construction and demolition waste suitable for concrete production", *Constr. Build.*  
434 *Mater.*, vol. 65, pp. 201–217, Aug. 2014.
- 435 [16] NF EN 197-1, "Cement - Part 1: composition, specifications and conformity criteria for  
436 common cements", Apr 2012.
- 437 [17] NF EN 196-1, "Methods of testing cement - Part 1: determination of strength", Sep. 2016.
- 438 [18] NF P18-452, "Concretes - Measuring the flow time of concretes and mortars using a  
439 workabilitymeter", Feb. 2017.
- 440 [19] NF EN 12350-6, "Testing fresh concrete - Part 6: density", Apr. 2012.
- 441 [20] NF EN 12390-2, "Testing hardened concrete - Part 2: making and curing specimens for  
442 strength tests", Apr. 2012.
- 443 [21] NF P18-459, "Concrete - Testing hardened concrete - Testing porosity and density", Mar.  
444 2010.
- 445 [22] NT BUILD 492, "Concrete, mortar and cement-based repair materials: Chloride migration  
446 coefficient from non-steady-state migration experiments", Nordtest.info, Nov. 1999.
- 447 [23] XP P18-463, "Concrete - Testing gas permeability on hardened concrete", Nov. 2011.
- 448 [24] NF EN 772-11, "Methods of test for masonry units - Part 11: Determination of water  
449 absorption of aggregate concrete, autoclaved aerated concrete, manufactured stone and  
450 natural stone masonry units due to capillary action and the initial rate of water absorption of  
451 clay masonry units", Aug. 2011.
- 452 [25] XP P18-458, "Tests for hardened concrete - Accelerated carbonation test - Measurement of  
453 the thickness of carbonated concrete", Nov. 2008.
- 454 [26] H. Hornain and G. Arliguie, *GranDuBé: grandeurs associées à la durabilité des bétons.*  
455 Chapter II.1, p305, Presses des Ponts, 2007.
- 456 [27] L. Bello, E. Garcia-Diaz, and P. Rougeau, "An original test method to assess water  
457 absorption/desorption of lightweight aggregates in presence of cement paste", *Constr. Build.*  
458 *Mater.*, vol. 154, pp. 752–762, Nov. 2017.
- 459 [28] R. Putra Jaya, B. H. Bakar, M. A. Megat Johari, and M. H. Ibrahim, "Strength and  
460 permeability properties of concrete containing rice husk ash with different grinding time",  
461 *Open Eng.*, vol. 1, pp. 103–112, Mar. 2011.
- 462 [29] S. Rasiyah, J. Kaabi, A. Mohammad, and Singh, "Permeability And Drying Of Pervious  
463 Concrete Pavers", Conference: ISEC-7, Honanulu, Hawaii, Jun. 2013.
- 464 [30] R. San Nicolas, *Approche performantielle des bétons avec métakaolins obtenus par*  
465 *calcination flash*. Toulouse 3 thesis, 2011.
- 466 [31] L. Evangelista and J. de Brito, "Durability performance of concrete made with fine recycled  
467 concrete aggregates", *Cem. Concr. Compos.*, vol. 32, no. 1, pp. 9–14, Jan. 2010.

- 468 [32] Z. Tahar, T.-T. Ngo, E. H. Kadri, A. Bouvet, F. Debieb, and S. Aggoun, "Effect of cement and  
469 admixture on the utilization of recycled aggregates in concrete", *Constr. Build. Mater.*, vol.  
470 149, pp. 91–102, Sep. 2017.
- 471 [33] V. W. Y. Tam, X. F. Gao, and C. M. Tam, "Microstructural analysis of recycled aggregate  
472 concrete produced from two-stage mixing approach", *Cem. Concr. Res.*, vol. 35, no. 6, pp.  
473 1195–1203, Jun. 2005.
- 474 [34] W. Li, J. Xiao, Z. Sun, S. Kawashima, and S. P. Shah, "Interfacial transition zones in recycled  
475 aggregate concrete with different mixing approaches", *Constr. Build. Mater.*, vol. 35, pp. 1045–  
476 1055, Oct. 2012.
- 477 [35] M. B. Leite and P. J. M. Monteiro, "Microstructural analysis of recycled concrete using X-ray  
478 microtomography", *Cem. Concr. Res.*, vol. 81, pp. 38–48, Mar. 2016.
- 479 [36] S. C. Angulo, P. M. Carrijo, A. D. Figueiredo, A. P. Chaves, and V. M. John, "On the  
480 classification of mixed construction and demolition waste aggregate by porosity and its impact  
481 on the mechanical performance of concrete", *Mater. Struct.*, vol. 43, no. 4, pp. 519–528, May  
482 2010.
- 483 [37] L. Evangelista and J. de Brito, "Criteria for the Use of Fine Recycled Concrete Aggregates in  
484 Concrete Production", Conference on the Use of Recycled Materials in Building and Structures,  
485 RILEM, Barcelona, Spain, Nov. 2004, (Academic paper (PDF) accessible by ResearchGate).
- 486 [38] M. S. de Juan and P. A. Gutiérrez, "Study on the influence of attached mortar content on  
487 the properties of recycled concrete aggregate", *Constr. Build. Mater.*, vol. 23, no. 2, pp. 872–  
488 877, Feb. 2009.
- 489 [39] A. Katz, "Properties of concrete made with recycled aggregate from partially hydrated old  
490 concrete", *Cem. Concr. Res.*, vol. 33, no. 5, pp. 703–711, May 2003.
- 491 [40] S.-C. Kou and C.-S. Poon, "Properties of concrete prepared with PVA-impregnated recycled  
492 concrete aggregates", *Cem. Concr. Compos.*, vol. 32, no. 8, pp. 649–654, Sep. 2010.
- 493 [41] A. K. Padmini, K. Ramamurthy, and M. S. Mathews, "Influence of parent concrete on the  
494 properties of recycled aggregate concrete", *Constr. Build. Mater.*, vol. 23, no. 2, pp. 829–836,  
495 Feb. 2009.
- 496 [42] H. Zhao, Q. Xiao, D. Huang, and S. Zhang, "Influence of Pore Structure on Compressive  
497 Strength of Cement Mortar", *Sci. World J.*, vol. 2014, p. e247058, Mar. 2014.
- 498 [43] J. de Brito and F. Alves, "Concrete with recycled aggregates: the Portuguese experimental  
499 research", *Mater. Struct.*, vol. 43, no. 1, pp. 35–51, Dec. 2010.
- 500 [44] A. Abbas *et al.*, "Quantification of the residual mortar content in recycled concrete  
501 aggregates by image analysis", *Mater. Charact.*, vol. 60, no. 7, pp. 716–728, Jul. 2009.

# Durability of mortars with leftover recycled sand

Manh Tan LE <sup>a,\*</sup>, Christelle TRIBOUT <sup>a</sup>, Gilles ESCADEILLAS <sup>a</sup>

<sup>a</sup> Université de Toulouse, UPS, INSA; LMDC (Laboratoire Matériaux et Durabilité des Constructions), 135, Avenue de Rangueil; F-31 077 Toulouse Cedex 04, France

\* Corresponding author. Tel +33665087813; E-mail address: mtle@insa-toulouse.fr.

Figure 1: Return of concrete from construction site .....	2
Figure 2: Particle size distributions (NS: Natural Sand; RS: Recycled Sand) .....	2
Figure 3: WA of different sands and their fractions by NF P 1097-6 method .....	3
Figure 4: Density of different sands and their fractions .....	3
Figure 5: Aggregate classification based on the relationship between water absorption and oven dried density (Silva et Al).....	3
Figure 6: SEM observation (Top: RS <sub>f</sub> Fraction 0 / 0.25 mm and bottom: RS <sub>c</sub> Fraction 1 / 4 mm) .....	4
Figure 7: Workability of the RS and CRS series .....	4
Figure 8: Density of the RS and CRS series in fresh state.....	5
Figure 9: Compressive strength of the RS and CRS series.....	5
Figure 10: Durability index for the RS mortars .....	6
Figure 11: Durability index for the CRS mortars .....	6
Figure 12: Relation between compressive strength and decrease of density of hardened mortars..	6
Figure 13: Schematic representation of sands (Black: natural sand; light grey: old cement paste; grey shaded: carbonated old cement paste; white: new cement paste) .....	6

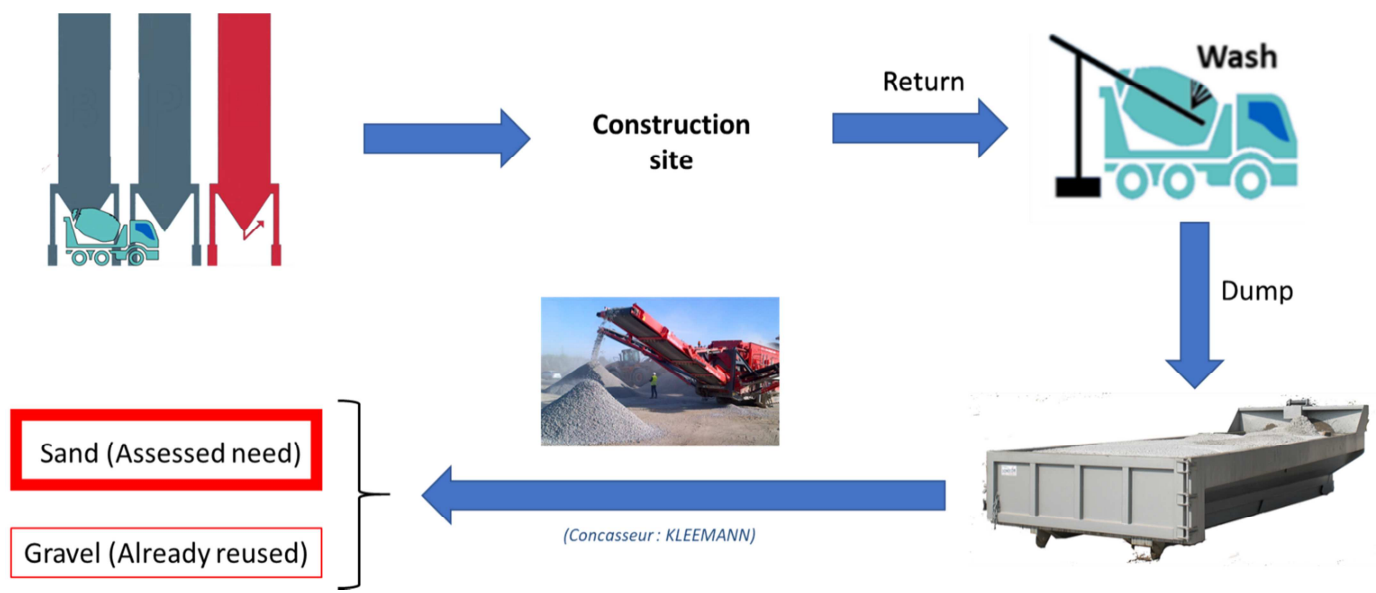


Figure 1: Return of concrete from construction site

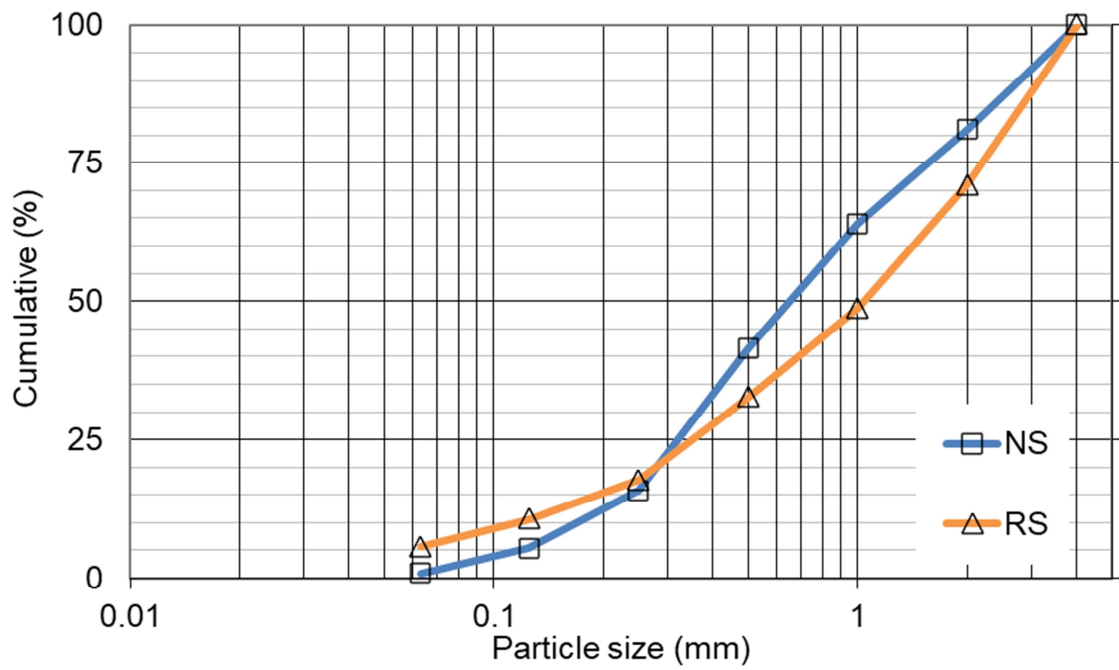


Figure 2: Particle size distributions (NS: Natural Sand; RS: Recycled Sand)

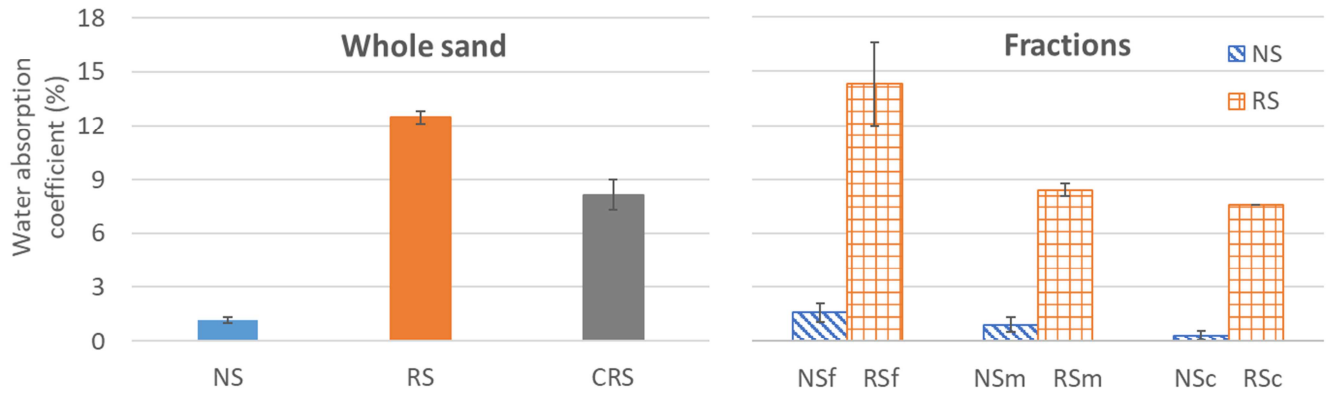


Figure 3: WA of different sands and their fractions by NF P 1097-6 method

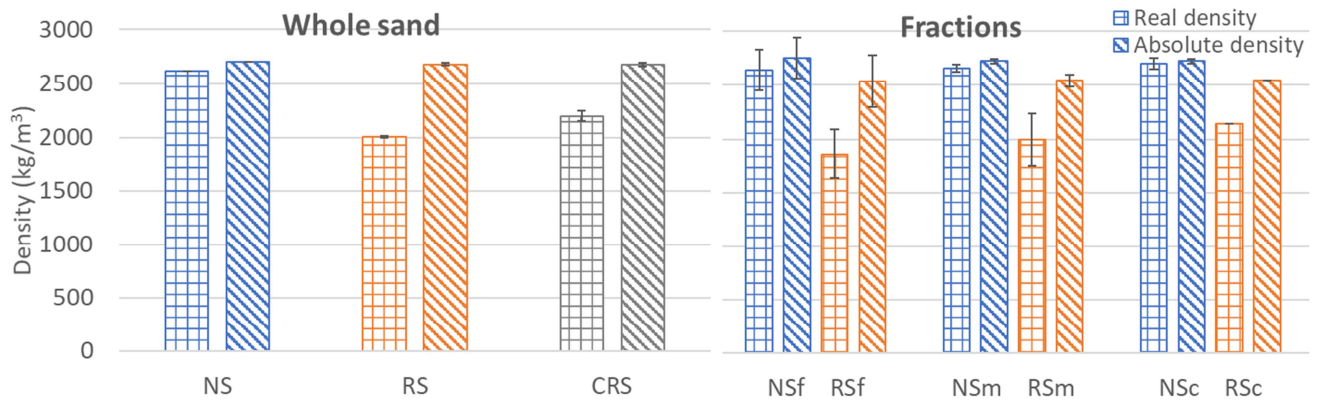


Figure 4: Density of different sands and their fractions

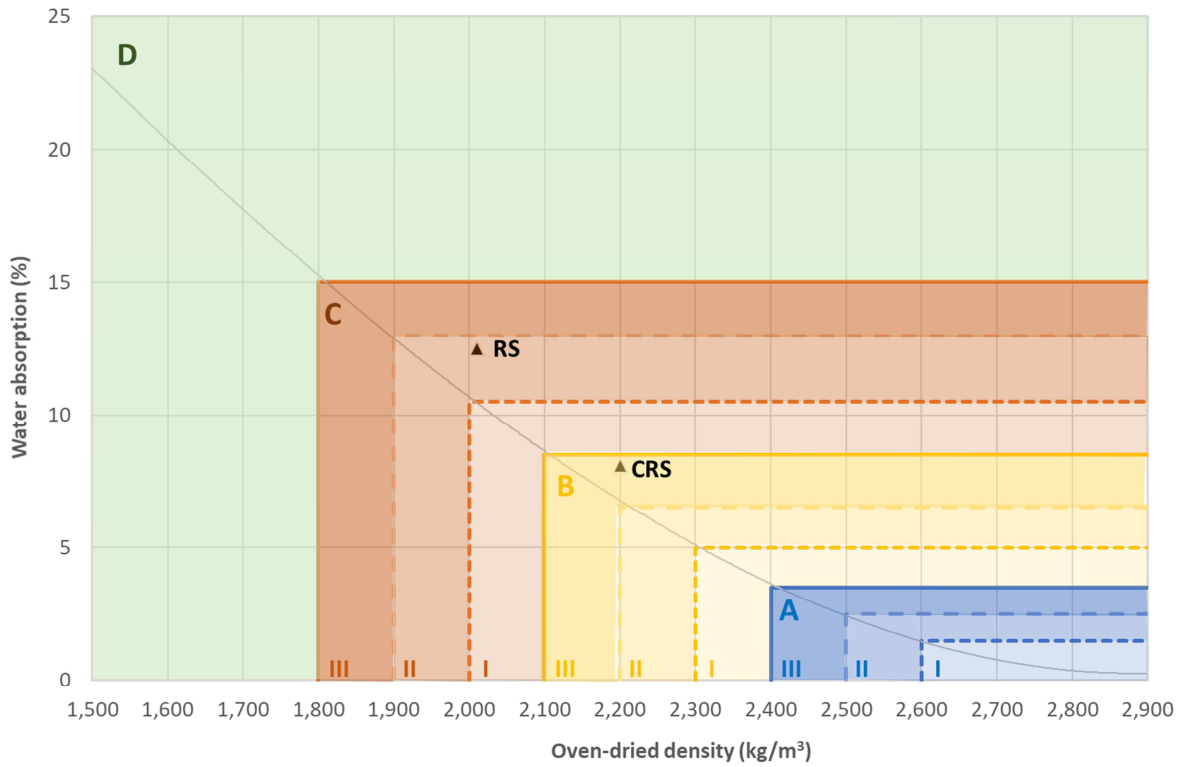


Figure 5: RS and CRS classification according to the aggregate codification proposed by Silva et al. [15]

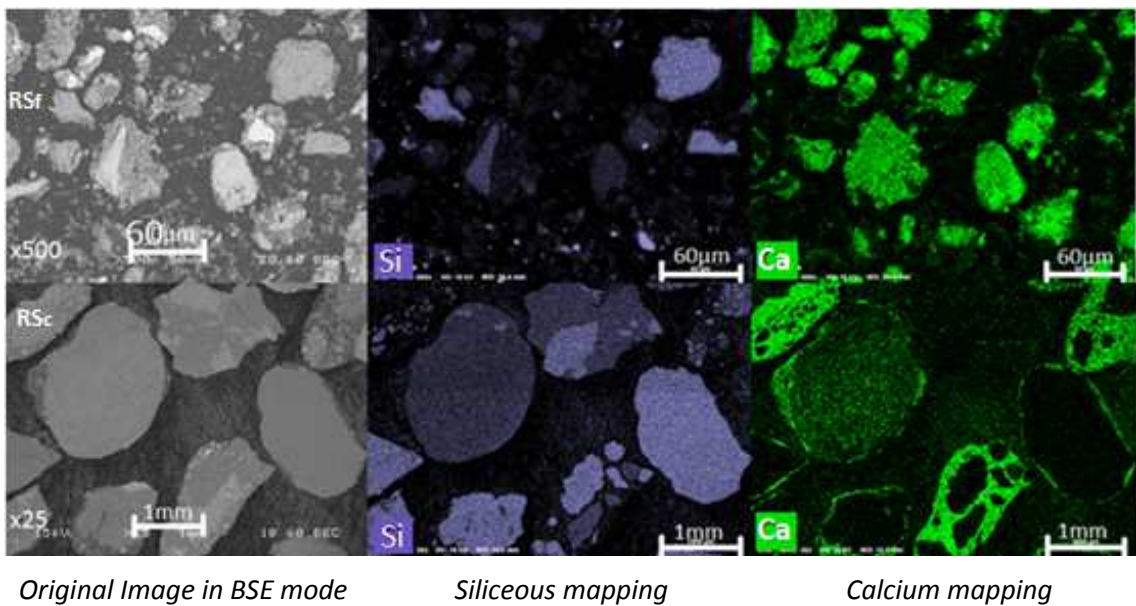


Figure 6: SEM observation (Top:  $RS_f$  Fraction 0 / 0.25 mm and bottom:  $RS_c$  Fraction 1 / 4 mm)

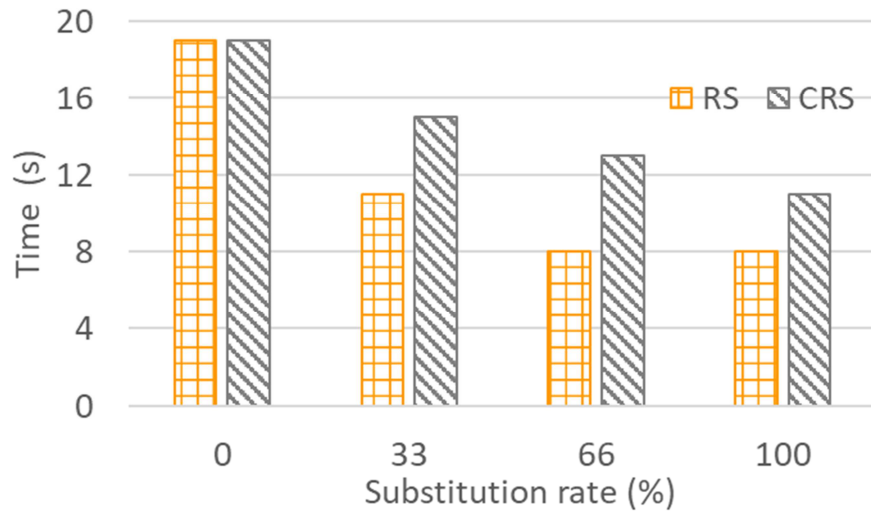


Figure 7: Workability of the RS and CRS series

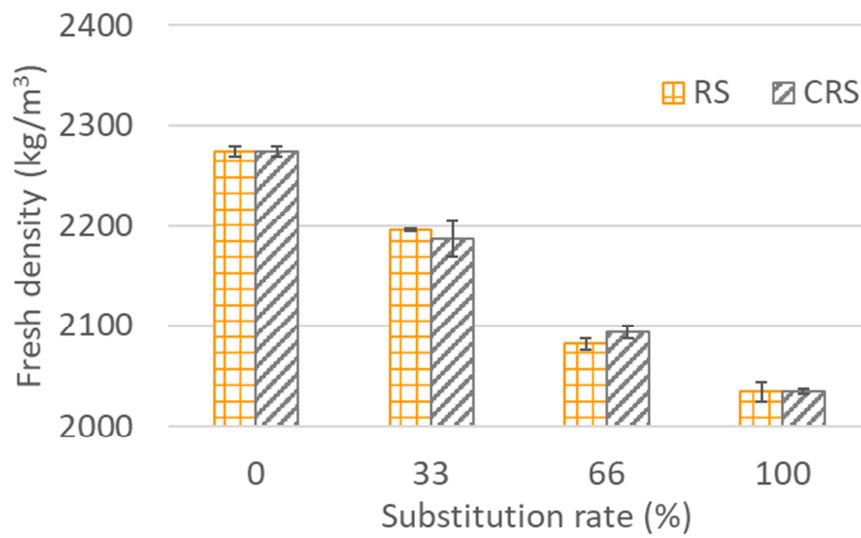


Figure 8: Density of the RS and CRS series in fresh state

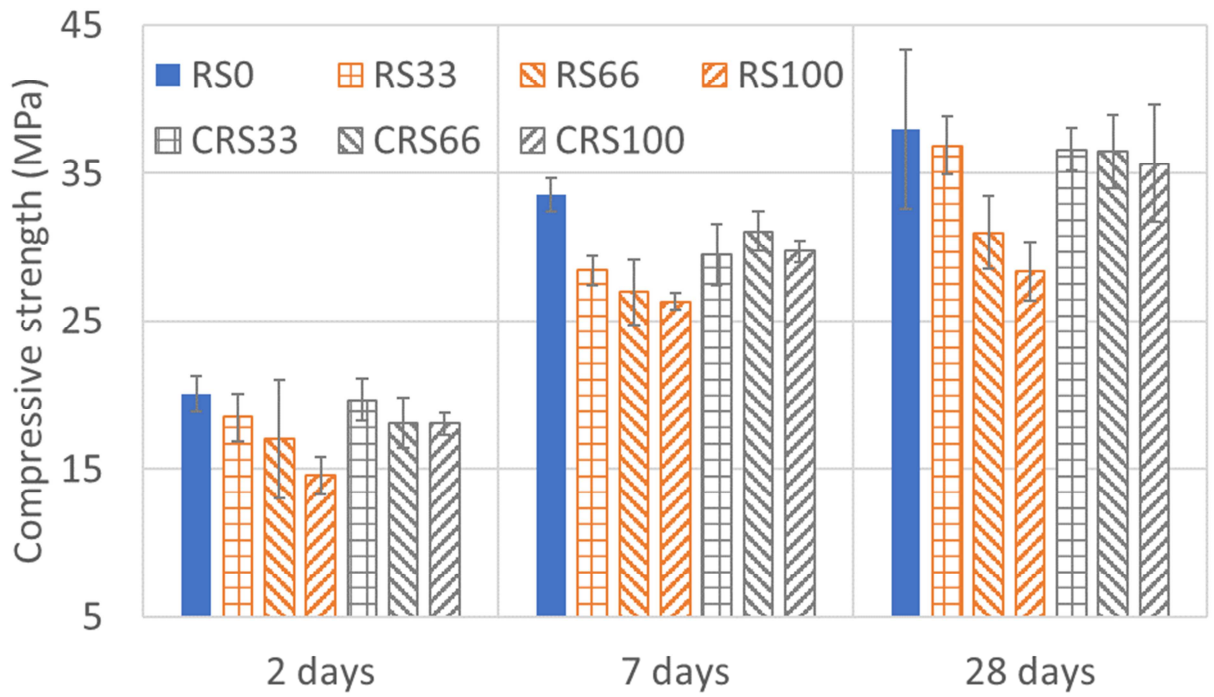


Figure 9: Compressive strength of the RS and CRS series

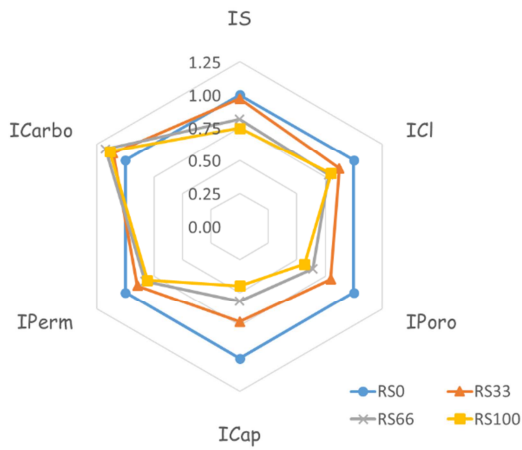


Figure 10: Durability index for the RS mortars

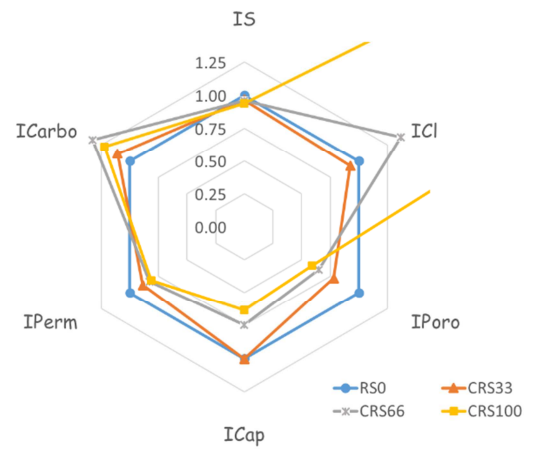


Figure 11: Durability index for the CRS mortars



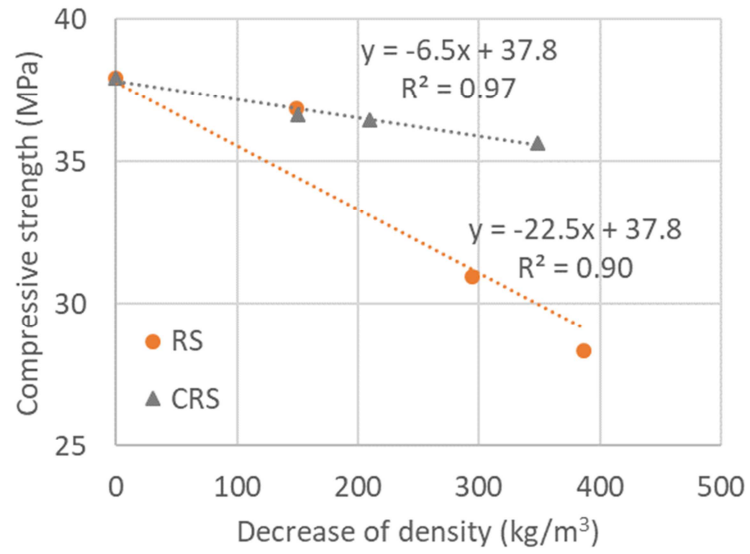


Figure 12: Relation between compressive strength and decrease of density of hardened mortars

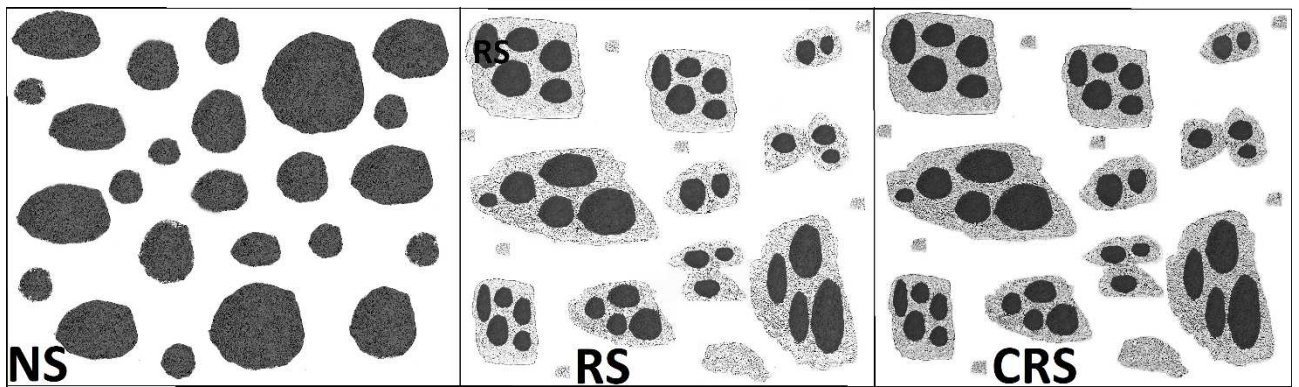


Figure 13: Schematic representation of sands (Black: natural sand; light grey: old cement paste; grey shaded: carbonated old cement paste; white: new cement paste)

# Durability of mortars with leftover recycled sand

Manh Tan LE <sup>a,\*</sup>, Christelle TRIBOUT <sup>a</sup>, Gilles ESCADEILLAS <sup>a</sup>

<sup>a</sup> Université de Toulouse, UPS, INSA; LMDC (Laboratoire Matériaux et Durabilité des Constructions), 135, Avenue de Rangueil; F-31 077 Toulouse Cedex 04, France

\* Corresponding author. Tel +33665087813; E-mail address: mtle@insa-toulouse.fr.

Oxides	CaO	SiO <sub>2</sub>	Al <sub>2</sub> O <sub>3</sub>	Fe <sub>2</sub> O <sub>3</sub>	MgO	SO <sub>3</sub>	K <sub>2</sub> O	Na <sub>2</sub> O	LOI
% mass	63.99	19.89	5.64	2.47	1.77	3.13	0.4	0.07	1.73
Bogue composition	C <sub>3</sub> S	C <sub>2</sub> S	C <sub>3</sub> A	C <sub>4</sub> AF					
% mass	53.7	17.9	9.5	6.9					

Table 1: Chemical and mineralogical compositions of ordinary Portland cement

Composition	Sand ratio (%)		Mass (kg)		Water for saturation (kg)	Cement (C) (kg)	Effective Water (W) (kg)	C/W	Theoretical density (kg/m <sup>3</sup> )
	NS	RS	NS	RS					
RS0	100	0	1703.0	0	19.8	333	222	0.67	2277.8
RS33	66	33	1135.3	435.5	67.5	333	222	0.67	2193.4
RS66	33	66	567.7	871.0	115.3	333	222	0.67	2109.0
RS100	0	100	0	1306.5	163.1	333	222	0.67	2024.6

	NS		CRS		(kg)	(kg)	(kg)	C/W	(kg/m <sup>3</sup> )
	NS	CRS	NS	CRS					
CRS33	66	33	1135.3	476.7	51.9	333	222	0.67	2218.9
CRS66	33	66	567.7	953.3	84.0	333	222	0.67	2160.0
CRS100	0	100	0	1430.0	116.1	333	222	0.67	2101.1

Table 2: Compositions of RS and CRS mortar series

	Loss of mass %		
	80-350	450-550	550-1000
Decomposition range (°C)	80-350	450-550	550-1000
Composition	C-S-H, Aft	Portlandite	Calcium carbonate
RS <sub>f</sub>	6.2	0.9	8.6
RS <sub>m</sub>	4.4	0.6	4.9
RS <sub>c</sub>	3.3	1.0	4.3

Table 3: Mass loss based on TG results for the different fractions of RS (%)

Durability	MORTAR :	Reference	With RS substitution			With CRS substitution		
	Unit	RS0	RS33	RS66	RS100	CRS33	CRS66	CRS100
Apparent density	kg/m <sup>3</sup>	2038.7 7.1	1889.3 7.1	1744.3 12.2	1652.3 3.9	1888.1 25.5	1773.9 9.0	1690.0 13.3
Porosity	%	19.4 0.1	24.4 0.3	30.3 0.3	34.3 0.6	24.9 0.2	29.9 0.2	32.9 0.1
Coefficient of chloride diffusion	E-11 m <sup>2</sup> /s	3.3 0.22	4.0 0.15	4.7 0.11	4.5 0.35	3.7 0.09	2.4 0.21	1.1 0.06
Permeability at 28 days	E-16 m <sup>2</sup>	66.7 15.2	104.0 6.0	155.0 8.9	229.0 15.1	182.0 17.7	241.0 10.1	284.0 44.0
Permeability at dry state	E-16 m <sup>2</sup>	113.0 9.4	198.0 25.8	298.0 16.6	343.0 18.2	208.0 25.9	302.0 1.1	338.0 47.3
Capillarity speed	kg/m <sup>2</sup> /min <sup>1/2</sup>	0.3 0.0074	0.4 0.0368	0.5 0.0069	0.6 0.0186	0.3 0.0316	0.4 0.0121	0.4 0.0117
Carbonation speed	mm/jour <sup>1/2</sup>	3.3 0.1	2.7 0.2	2.7 0.1	2.8 0.1	2.8 0.2	2.5 0.1	2.8 0.2

Standard deviation

Table 4: Durability of RS and CRS mortar series

Criteria in comparison with NS		RS	CRS
Basic characteristics	Fresh density (3.2.2)	-	-
	Workability (3.2.1)	++++	+++
	Water Absorption (2.1.1) <b>(1)</b>	----	---
	Hardened density (3.3.1)	--	--
Durability	Strength (3.2.3)	--	-
	Porosity (3.3.1) <b>(2)</b>	---	--
	Air permeability (3.3.3)	-	-
	Capillarity (3.3.4)	---	--
	Carbonation (3.3.5) <b>(3)</b>	+	++
	Chloride ion migration (3.3.2)	-	++++

Table 5: Variation of the measured parameters for RS and CRS mixtures: what effect? ('+' positive effect; '-' negative effect; 'X' slight; 'XX' average; 'XXX' significant; 'XXXX' strong).